Dear Author

Please use this PDF proof to check the layout of your article. If you would like any changes to be made to the layout, you can leave instructions in the online proofing interface. Making your changes directly in the online proofing interface is the quickest, easiest way to correct and submit your proof. Please note that changes made to the article in the online proofing interface will be added to the article before publication, but are not reflected in this PDF proof.

If you would prefer to submit your corrections by annotating the PDF proof, please download and submit an annotatable PDF proof by clicking here and you'll be redirected to our PDF Proofing system.

ELSEVIER

Predestinitive Role of Cardiac Ganglia on Heart Life Expectancy in Rabbits After Brain Death Following Subarachnoid Hemorrhage: An Experimental Study

Mehmet Dumlu Aydin[a,*], Mahmut Acikel[b], Nazan Aydin[c], Muhammed Enes Aydin[d], Ali Ahiskalioglu[d], Canan Atalay[d], Elif Oral Ahiskalioglu[d], Fazlı Erdogan[e], and Sare Sipal[f]

[a]Ataturk University, Medical Faculty, Department of Neurosurgery, Erzurum, Turkey; [b]Ankara Higher Education and Research Hospital, Department of Cardiology, Ankara, Turkey; [c]Uskudar University, Medical Faculty, Department of Psychiatri, Erzurum, Turkey; [d]Ataturk University, Medical Faculty, Department of Anesthesiology and Reanimation, Erzurum, Turkey; [e]Ataturk Training and Research Hospital, Department of Pathology Ankara, Turkey; and [f]Ataturk University, Medical Faculty, Department of Pathology, Erzurum, Turkey

ABSTRACT

Background. Cardiac ganglia are rechargeable batteries of the heart. The essential role of cardiac ganglia on cardiac life expectancy has not been examined following brain death. The aim of this study was to determine cardiac ganglia numbers and neuron density following subarachnoid hemorrhage (SAH).

Methods. Twenty-five hybrid rabbits were grouped as control (n = 5), sham (n = 5), and SAH (n = 15). The SAH groups' animals were subjected to injections of lethal dose of 2.00 cc autologous blood into their cisterna magna until linear EEG was obtained. The hearts of all animals were extracted following intracardiac formalin injection and examined. Cardiac ganglia and normal/degenerated neuron densities of cardiac neurons were recorded.

Results. The mean volume of normal neuron density of ganglia was 6.980 ± 830/mm^3, and the degenerated neuron density of ganglia was 3 ± 1/mm^3 in the control group, 6134 ± 712/mm^3; 23 ± 9/mm^3 in the sham group, 3456 ± 589; 1161 ± 72/mm^3 in the surviving group; and 1734 ± 341/mm^3, 4259 ± 865/mm^3 in the dead animals in the SAH group. The algebraic results of heart work capacity (Wh) were estimated as 1375 ± 210 Wh in the control group, 1036 ± 225 in the sham group, 800 ± 110 Wh in the surviving group, and < 100 ± 20 in the dead animals in the SAH group. Degenerated cardiac neuron density/Wh correlation is statistically meaningful between the dead in the SAH group versus the SAH-surviving, sham, and control groups ($P < .0005$).

Conclusions. Normal cardiac ganglia numbers and/or cardiac ganglia neuron density may be related to cardiac survival following brain death after subarachnoid hemorrhage.

CARDIAC death is described as loss of myocardial vitality represented by a linear electrocardiogram (ECG). Cardiac control is regulated by wide neural networks included the intrinsic cardiac ganglia, intrathoracic extracardiac ganglia, sympathetic cervical ganglia, spinal cord, brainstem, and higher centers [1]. Vagal cardiac efferents project to cardiac ganglia and regulate heart rate [2]. The vagus nerve is a very important regulator in many emotional and physical conditions. Vagus pathway paralysis may result in indirect sympathetic overactivity and causes depletion of the heart's reserves [3]. The cardiac nerves formed a ganglionated neural plexus in epicardial fat pads, vena cavae, and cardiac nodes [4], which prevent myocardial ischemia [5].

The heart is innervated sympathetically by bilateral cervical ganglia [6]. Cervicothoracic sympathetic chain

*Address correspondence to Mehmet Dumlu Aydin, Ataturk University, Medical Faculty, Department of Neurosurgery, Erzurum, Turkey. Tel: 90 532 322 83 89. E-mail: nmda11@hotmail.com

0041-1345/19
https://doi.org/10.1016/j.transproceed.2019.09.011

FLA 5.6.0 DTD ■ TPS29477_proof ■ 3 December 2019 ■ 4:50 am ■ ce

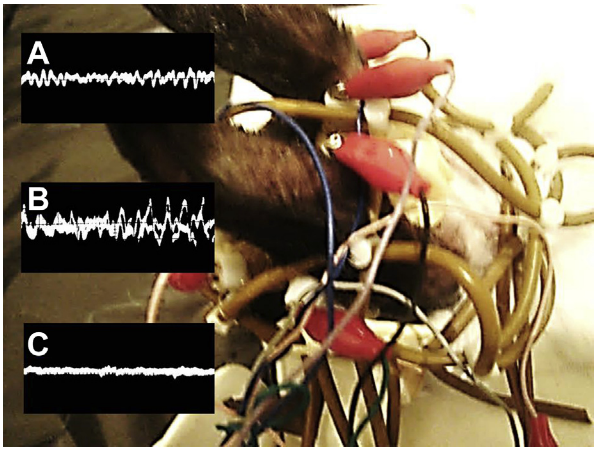

Fig 1. EEC recording method is seen in a rabbit. Normal EEG **(A)**, abnormal EEC in SAH created animal **(B)**, and brain death showing EEG **(C)**.

web 4C/FPO

modulate sympathetic innervation of heart [7]. Low density or a high proportion of degenerated neurons of stellate ganglion may be responsible for bradycardia [8]. The high neuron density of stellate ganglion causes heart conduction systems to degenerate and atrial fibrillation following myocardial infarction [9–13]. Carotid bodies/sinuses/sympathetic chain atrophy renormalizes by retrograde blood flow and prevents acidosis [14–16]. Sympathetic overactivation results in myocardial damage and even contraction band necrosis following SAH [17–19]. Low neuron density of cardiac ganglia may be dangerous by its decreased supportive effects for the higher cardiac energy, resulting in chronic heart disease. Ischemic time of a transported heart is a very important in regard to heart viability. High neuron density of cardiac ganglia may have beneficial effects for cardiac hyperactivity following brain death. Epicardial ganglia morphology and functions are very important for heart survival after brain death. We hypothesized that vagal nerves recharge intrinsic cardiac ganglia and prolong the life of the heart. During the donor harvesting procedure, applied vagotomy could cause denervation injury of cardiac ganglia and decrease heart life expectancy. In the future, mini-vagal stimulators could be used to charge cardiac ganglia to maintain heart functions until donor preparation for transplantation is complete.

MATERIALS AND METHODS

This study was conducted on a total of 25 New Zealand white rabbits. The experimental protocols were approved by Ataturk University Ethics Committee guidelines. Twenty-five hybrid rabbits were grouped as control ($n = 5$), sham ($n = 5$), and SAH ($n = 15$).

Experimental Protocol

To examine brain death, light reflexes, pupillary answers to light, pupil diameters, electroencephalogram (EEG), and electrocardiogram (ECG) findings were recorded. Pupil diameters and fundoscopic examinations were done in light and dark environments for 3 times a day for 2 days prior to inducing SAH. Linear EEG and ECG were considered as brain and heart death.

Five animals were used for the anatomic and histopathological examinations of the cardiac ganglia. Anesthesia was administered with isoflurane applied by a face mask, and 0.2 mL/kg of the anesthetic combination, given intramuscularly (ketamine HCl, 150 mg/1.5 mL; Xylazine HCl, 30 mg/1.5 mL; and distilled water, 1 mL), was used for anesthesia. Autologous blood (2 mL) taken from the auricular artery was injected into the cisterna magna in the SAH group; 2 mL of saline was given to the sham group using a 22-gauge needle. Animals were followed for 5 days to obtain linear EEGs and ECGs; the animals were then killed. The brains, vagal nerves with their ganglions, and hearts were extracted and stored in 10% formalin solutions.

EEG WAVE RECORDINGS

Under anesthesia, all craniums were shaved and EEG electrodes implanted (Fig 1).

ECG Wave Recordings and Heart Death Description

To decide cardiac death, the surface area between ECG waves and isoelectric line were accepted as heart force (Fh); long of ECGs between P and T waves were accepted as heart way (Lh); and Fh $\times$ Lh were accepted as heart work, describing formula designed by ourselves (DADA equation). The algebraic criteria of cardiac death were accepted as $Wh = Fh \times Lh = 0$ because linear form ECGs have no surface area and no have long. The calculation formulas are shown in Fig 3.

ANATOMIC EXAMINATION

All brain stems, vagal nerves, and cardiac ganglia of all animals were examined for anatomopathological characteristics.

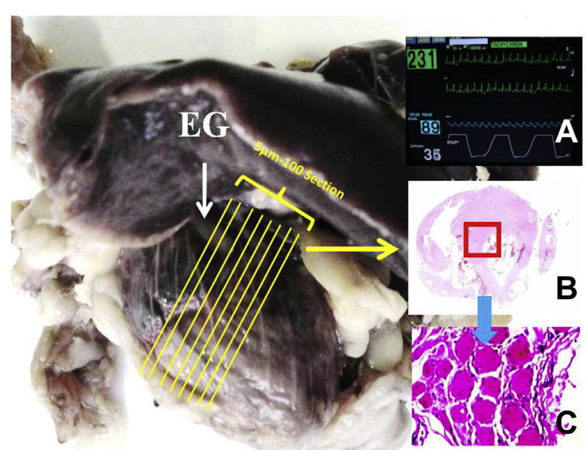

web 4C/FPO

Fig 2. ECG findings of a normal rabbit **(A)**, macroscopic appearance of a heart fixed with formalin and section levels to detect cardiac ganglia (EG) (yellow lines-base), histologic appearance of heart tissue at the section level and location of EG (LM, H&E, x2) **(B)**, and cardiac ganglia neurons (LM, H&E, x10) **(C)**.

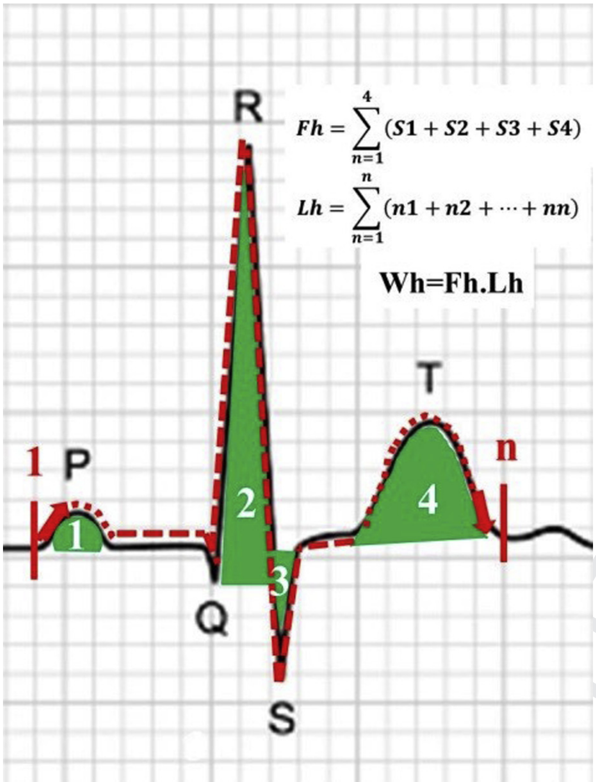

Fig 3. Calculation of heart work values and decision of cardiac death with DADA equation.

QUANTITATIVE EXAMINATION OF CARDIAC GANGLIA

All brain stems were sectioned at 2-mm distances with the vagal complex (roots and ganglia), and heart sections taken from sinoatrial/atrioventricular node levels were embedded in paraffin blocks. Cardiac ganglia located around the superior vena cavae were hindered by fatty tissue in the epicardium. To assess the ganglia numbers and their neurons numbers within the ganglia, 5 µm-thick serial sections were examined. To estimate the neuronal density of the vagal and cardiac ganglia. The tissues were stained with hematoxylin and eosin (H&E) and Masson's trichrome and tunnel methods, and the stereological and Cavalieri methods were used to evaluate the neuronal density of these ganglia as our previous studies [3]. The numbers of normal and degenerated neurons in the cardiac ganglia of each animal were counted.

ELECTROPHYSIOLOGICAL AND HISTOPATHOLOGICAL RESULTS

Figure 1 shows the EEC recording method. Normal EEGs and abnormal EECs in the SAH group created animal and brain death, shown on the EEGs. ECG findings of a normal rabbit, the macroscopic appearance of a heart fixed with formalin and section levels to detect cardiac ganglia, and the histologic appearance of heart tissue at the section level and location of cardiac ganglia neurons are shown in Fig 2. Calculation of heart work values and the decision of cardiac death using the DADA equation are shown in Fig 3. Figure 4 shows normal ECGs of normal rabbits, cardiac ganglia, and magnified representation. Stereological cell counting of the cardiac ganglia in a rabbit shown in Figs 5A and 5B. The abnormal ECG, degenerated cardiac ganglia neurons, and magnified representation of a living rabbit were nearly normal (Fig 6). Figure 7 shows that degenerated cardiac ganglia neurons in myocardium, magnified representation, and abnormal ECG in a dead rabbit have less normal and more degenerated neurons than included in intracardiac ganglia. Degenerated epicardial ganglia neurons and their magnified representation with apoptotic neurons; coronary artery, vagal nerves, and myocytes in normal animals; and normal and degenerated axons of vagal nerves in a dead rabbit have less normal and more degenerated neurons than included in intracardiac ganglia (Fig 8).

NUMERICAL RESULTS

One animal of the sham group and 3 animals of the SAH group died in the first week. Six animals stay alive with a low-level Glasgow Coma Score (< 10). The cardiac ganglia number was more than 8 in the surviving animals and less than 5 in the dead animals. The mean normal/degenerated neuron density was estimated as: 6.980 ± 830/mm^3; 3 ± 1/mm^3 in the control group; 6134 ± 712/mm^3; 23 ± 9/mm^3 in the sham group, 3456 ± 589; 1161 ± 72/mm^3 in the surviving group; and 1734 ± 341/mm^3, 4259 ± 865/mm^3 in the dead animals in the SAH group following brain death. The algebraic results of heart work capacity (Wh) were estimated as 1375 ± 210 Wh in the control group, 1036 ± 225 in the sham group, 800 ± 110 Wh in the surviving group, and < 100 ± 20 in the dead animals in the SAH group. Numerical results and statistical analysis are shown in Table 1. Degenerated cardiac neuron density/Wh

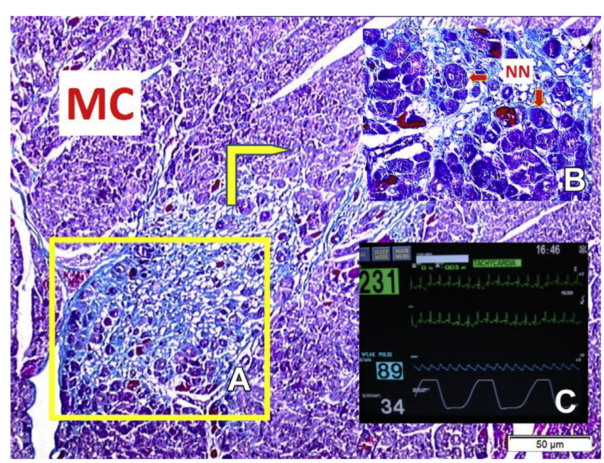

Fig 4. Normal ECG of normal rabbits **(A)**, cardiac ganglia **(B)**, and magnified representation **(C)** (MTC, LM, x4/A; x10).

web 4C/FPO

web 4C/FPO

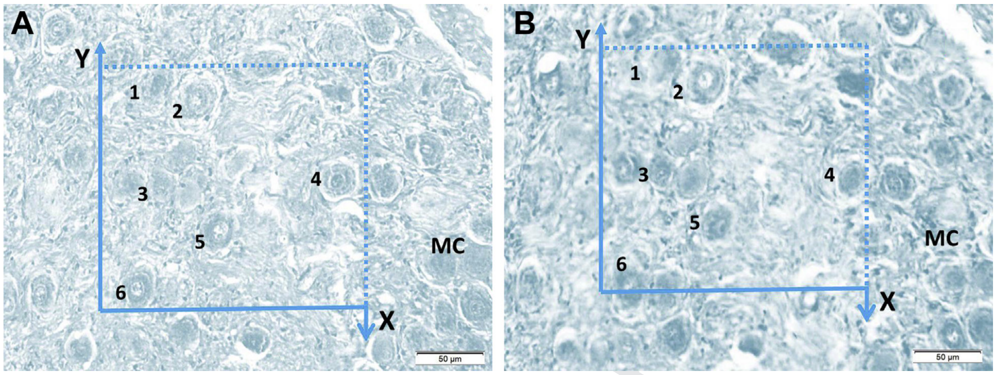

Fig 5. **(A, B)** Stereological cell counting method used for the cardiac ganglia neuron density of rabbit. Same fields of micrographs **(A, B)** were obtained from 2 parallel, consecutive, thin sections divided by a 5 μm distance. The upper-right lines of frames show the inclusion lines, and the bottom-left lines are exclusion lines. The neuronal nucleoli crossing by the inclusion lines are not counted, and the nucleoli not crossing the inclusion lines were counted as dissector particles. The neuron number of 2 dissectors pairs each specimen volume obtained from the counting frames and distance between the consecutive sections. The numerical density of the neurons is calculated as NvGN =ΣQ – GN/txA. In this application, the nucleoli marked with "4-6" are dissector particles in **(A)**. Section **(B)** shows them as they disappeared. The nucleoli marked with "1, 2, 3" are not a dissector particle in **(A)**. Section **(B)** shows "1, 2, 3" as it disappeared (LM, Nissl Stain, X10).

correlation is statistically meaningful between the dead in the SAH group versus the SAH-surviving, sham, and control groups ($P < .0005$).

STATISTICAL ANALYSIS

All values are expressed as the mean ± standard deviation. The differences between the degenerated neuron densities of cardiac ganglia of each group were compared statistically. A 1-way analysis of variance followed by Bonferroni's post hoc test was used to determine significant differences between the cardiac neuron density and Wh values whose differences were considered to be significant at $P < .05$.

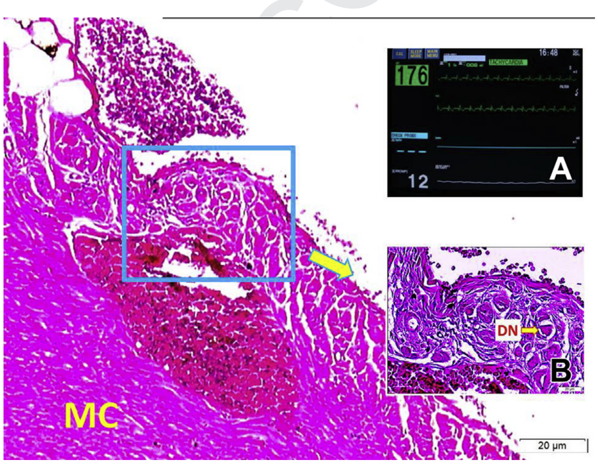

Fig 6. Abnormal ECG **(A)**, degenerated cardiac ganglia neurons (LM, H&E, x4/Base); magnified representation (LM, H&E, x10) of a living rabbit was nearly normal.

DISCUSSION

Cardiac rhythm is regulated via a rich neuronal network web through the intrinsic ganglia and extracardiac ganglia, stellate, middle cervical and superior cervical ganglia, spinal cord, brainstem, and higher brain centers [1]. Vagal axons in cardiac ganglia make a web between the cardiac ganglia and muscles [2]. The atrial cardiac nerves form a wide ganglionated neural plexus and distribute through the parietal pericardium and epicardium and then beyond the superior vena cava, heart hilum, and right atrium and dorsal surface of the right auricle. These ganglia communicate with the

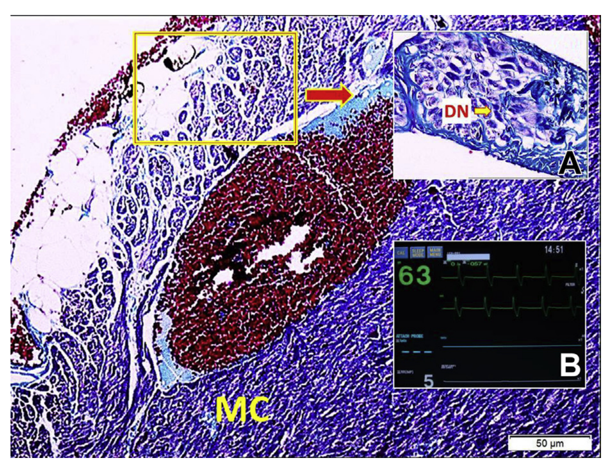

Fig 7. Degenerated cardiac ganglia neurons in myocardium (LM, H&E, x4/Base), magnified representation (LM, H&E, x10/A), and abnormal ECG **(B)** in a dead rabbit have less normal and more degenerated neurons included in the intracardiac ganglia.

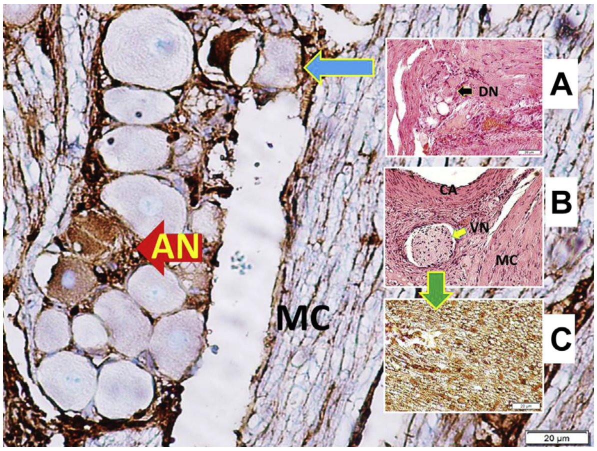

Fig 8. Degenerated epicardial ganglia neurons (LM, H&E, x20) **(A)** and its magnified representation with apoptotic neurons (AN) (LM, Tunnel, x20/Base); coronary artery (CA), vagal nerve (VN), and myocytes (MC) in a normal animal (LM, H&E, x10) **(B)**; and normal (dark) and degenerated (clear) axons of vagal nerves in a dead rabbit have less normal and more degenerated neurons included in the intracardiac ganglia (LM, S-100, x10).

epicardial nerves around the coronary arteries and arterial part of the heart hilum [4]. This network plays an important preventive role in the intrinsic cardiac nervous system for myocardial ischemic preconditioning [5].

The essential regulator of heart rhythm is the vagal network consisting of efferent and afferent pathways. Neurodegeneration of the nodose ganglia following SAH may cause cardiac arrest. Vagal paralysis induces sympathetic tachycardia and depletion of the heart's reserves [3]. Carotid artery stenosis induces bradycardia secondary to decreased neuron density in stellate ganglion ischemia during SAH [9]. Cardiac vagal activity is diminished in SAH and causes arrhythmias. Vagal network ischemia causes coronary vasospasm-induced cardiac arrest after SAH [6]. Stellate ganglion ischemia-related indirect vagal hyperactivity may cause heart rhythm disturbances following stenoocclusive carotid artery diseases. Stenoocclusive carotid artery diseases produce craniocerebral tissue ischemia [20], including sympathetic cervical and vagal nerve networks. Bilateral common carotid artery ligation causes retrograde blood flow [14] and protects stellate ganglia and carotid bodies [9,14]. Psychosocial stressors are risk factors for sudden cardiac death possibly due to the vagal effect [21]. Vagal ischemia augments cardiac inflammation and accelerates cardiac death during SAH [22].

Stellate ganglion represents the main sympathetic input to the heart [7]. Stellate ganglion impulses cause vasospasm in pial arteries [23]. Superior cervical ganglion resection causes heart rhythm variables [24]. The stellate ganglia convey cardiac pain and cardiac nociceptive transmission [25]. Low-density or high degenerated neurons of stellate ganglion may be responsible for bradycardia [8]. Stellate ganglion blockage inhibits sympathetic neural excitation on internal organs [26]. Sympathetic nerve activation is arrhythmogenic [27] mediated by contraction of the smooth muscle in the coronary artery [28]. Stellate ganglion stimulation induces a rise of blood pressure causing cardiovascular diseases [29]. Sympathetic hyperinnervation causes axon degeneration in heart conduction systems [10]. Ganglionated plexuses ablation during atrial fibrillation is a useful method [30]. Bilateral cardiac sympathetic denervation reduces ventricular tachyarrhythmias in infarcted hearts [31]. Sympathetic carotid baroreflex stimulation can have a potential antiarrhythmogenic effect [32] atrial fibrillation [11] and myocardial infarction [12]. Carotid bodies/sinuses go into complete atrophy in carotid stenosis [14] and develop retrograde blood flow, which can be ameliorated by sympathetic chain and carotid body degeneration [15] and prevent blood/cerebrospinal fluid acidosis and cardiac necrosis [16] and mononuclear cell infiltration [33]. Cardiac parasympathetic nerve activity causes ictal bradyarrhythmia, cardiac asystole, and sudden deaths of epileptic patients [34].

The pathophysiological mechanism of cardiac pathologies are unsettled in SAH. Increased sympathetic nerve stimulation or parasympathetic dysfunctions are responsible for cardiac injury and arrest. Excessive catecholamine release during parasympathetic dysfunction may allow cardiac inflammation, leading to myocardial cell death [18,35].

CONCLUSION

Epicardial ganglia neuron density plays a significant role in the regulation of heart rhythm and life expectancy. Low neuron density of epicardial ganglia should be considered a dangerous factor in the pathogenesis of severe bradycardia development in heart disease. Low neuron density of epicardial ganglia may be dangerous due to its decreased supportive effects for the higher cardiac energy required by chronic heart disease. High neuron density of epicardial ganglia may prolong heart survival following brain death.

Table 1. Estimation of Normal/Degenerated Neuron Density and Heart Work Capacity

	Group Control	Group Sham	Group SAH-Surviving	Group SAH-Dead
Normal neuron density (mm^3)	6.980 ± 830	6134 ± 712*	3456 ± 589 $^{\dagger,\beta}$	1734 ± 341$^{\beta}$
Degenerated neuron density (mm^3)	3 ± 1	23 ± 9*	1161 ± 72$^{\dagger,\beta}$	4259±865$^{\beta}$
Heart Work Capacity (Wh)	1375 ± 210	1036 ± 225*	800 ± 110 $^{\dagger,\beta}$	<100 ± 20 $^{\beta}$

‡$P < .0005$ between group sham vs SAH-surviving.
§$P < .0005$ between group SAH dead vs groups SAH-surviving, sham, control.
*$P < .001$ between group control vs sham.
†$P < .0001$ between group control vs SAH-surviving.

FUTURE INSIGHTS

We theorized that vagal nerves charge intrinsic cardiac ganglia and prolong the life of the heart. Mini-vagal stimulators could be used for charging cardiac ganglia to maintain heart functions until donor preparation for transplantation is complete.

REFERENCES

[1] Ardell JL, Armour JA. Neurocardiology: structure-based function. Compr Physiol 2016;6:1635–53.

[2] Cheng ZJ. Vagal cardiac efferent innervation in F344 rats: effects of chronic intermittent hypoxia. Autonomic Neurosci 2017;203:9–16.

[3] Aydin MD, Kanat A, Yilmaz A, et al. The role of ischemic neurodegeneration of the nodose ganglia on cardiac arrest after subarachnoid hemorrhage: an experimental study. Exp Neurol 2011;230:90–5.

[4] Pauza DH, Skripka V, Pauziene N, Stropus R. Anatomical study of the neural ganglionated plexus in the canine right atrium: implications for selective denervation and electrophysiology of the sinoatrial node in dog. Anat Rec 1999;255:271–94.

[5] Pickard JMJ, Burke N, Davidson SM, Yellon DM. Intrinsic cardiac ganglia and acetylcholine are important in the mechanism of ischaemic preconditioning. Basic Res Cardiol 2017;112:11.

[6] Yolas C, Kanat A, Aydin MD, et al. Unraveling of the effect of nodose ganglion degeneration on the coronary artery vasospasm after subarachnoid hemorrhage: an experimental study. World Neurosurg 2016;86:79–87.

[7] Cavalcanti RA, da Pureza DY, de Melo MP, et al. Low-intensity treadmill exercise-related changes in the rat stellate ganglion neurons. J Neurosci Res 2009;87:1334–42.

[8] Shao LJ, Liang SD, Li GL, Xu CS, Zhang CP. Exploration of P2X3 in the rat stellate ganglia after myocardial ischemia. Acta histochemica 2007;109:330–7.

[9] Onen MR, Yilmaz I, Ramazanoglu L, et al. Rational roots of sympathetic overactivity by neurogenic pulmonary edema modeling arising from sympathyco-vagal imbalance in subarachnoid hemorrhage: an experimental study. World Neurosurg 2016;92:463–70.

[10] Lorentz CU, Parrish DC, Alston EN, et al. Sympathetic denervation of peri-infarct myocardium requires the p75 neurotrophin receptor. Exp Neurol 2013;249:111–9.

[11] Hou Y, Hu J, Po SS, et al. Catheter-based renal sympathetic denervation significantly inhibits atrial fibrillation induced by electrical stimulation of the left stellate ganglion and rapid atrial pacing. PloS One 2013;8:e78218.

[12] Piccirillo G, Moscucci F, D'Alessandro G, et al. Myocardial repolarization dispersion and autonomic nerve activity in a canine experimental acute myocardial infarction model. Heart Rhythm 2014;11:110–8.

[13] Du XJ, Riemersma RA, Fox KA, Dart AM. Propranolol and lidocaine inhibit neural norepinephrine release in hearts with increased extracellular potassium and ischemia. Circulation 1993;88:1885–92.

[14] Aydin MD, Ozkan U, Gundogdu C, Onder A. Protective effect of posterior cerebral circulation on carotid body ischemia. Acta Neurochir 2002;144:369–72.

[15] Eseoglu M, Yilmaz I, Karalar M, et al. The role of sympathectomy on the regulation of basilar artery volume changes in stenoocclusive carotid artery modeling after bilateral common carotid artery ligation: an animal model. Acta Neurochir 2014;156:963–9.

[16] Ozmen S, Altinkaynak K, Aydin MD, et al. Toward understanding the causes of blood pH irregularities and the roles of newly described binuclear neurons of carotid bodies on blood pH regulation during subarachnoid hemorrhage: experimental study. Neuropathology 2019;39:259–67.

[17] Hawkins WE, Clower BR. Myocardial damage after head trauma and simulated intracranial haemorrhage in mice: the role of the autonomic nervous system. Cardiovasc Res 1971;5:524–9.

[18] van den Bergh WM, Algra A, Rinkel GJ. Electrocardiographic abnormalities and serum magnesium in patients with subarachnoid hemorrhage. Stroke 2004;35:644–8.

[19] Kawahara E, Ikeda S, Miyahara Y, Kohno S. Role of autonomic nervous dysfunction in electrocardio-graphic abnormalities and cardiac injury in patients with acute subarachnoid hemorrhage. Circ J 2003;67:753–6.

[20] Oldendorf WH. Trophic changes in the arteries at the base of the rat brain in response to bilateral common carotid ligation. J Neuropathol 1989;48:534–47.

[21] Skinner JE. Regulation of cardiac vulnerability by the cerebral defense system. J Am Coll Cardiol 1985;5:88b–94b.

[22] Tracey KJ. The inflammatory reflex. Nature 2002;420:853–9.

[23] Cohen Z, Bovento G, Lacombe P, Seylaz J, MacKenzie ET, Hamel E. Cerebrovascular nerve fibers immunoreactive for tryptophan-5-hydroxylase in the rat: distribution, putative origin and comparison with sympathetic noradrenergic nerves. Brain Res 1992;598:203–14.

[24] Sato T, Sato S, Suzuki J. Correlation with superior cervical sympathetic ganglion and sympathetic nerve innervation of intracranial artery-electron microscopical studies. Brain Res 1980;188:33–41.

[25] Zhang C, Li G, Liang S, et al. Myocardial ischemic nociceptive signaling mediated by P2X3 receptor in rat stellate ganglion neurons. Brain Res Bull 2008;75:77–82.

[26] Chen Y, Xie Y, Xue Y, Wang B, Jin X. Effects of ultrasound-guided stellate ganglion block on autonomic nervous function during CO2-pneumoperitoneum: a randomized double-blind control trial. J Clin Anesth 2016;32:255–61.

[27] Yu HG, Chung H, Yoon TG, Yum KW, Kim HJ. Stellate ganglion block increases blood flow into the optic nerve head and the peripapillary retina in human. Auton Neurosc 2003;109:53–7.

[28] Hagestad EL, Verrier RL. Delayed myocardial ischemia following the cessation of sympathetic stimulation. Am Heart J 1988;115:45–53.

[29] Cheng LJ, Li GP, Li J, Chen Y, Wang XH. Effects of fluvastatin on characteristics of stellate ganglion neurons in a rabbit model of myocardial ischemia. Chin Med J 2016;129:549–56.

[30] Lemery R, Ben-Haim S, Wells G, Ruddy TD. I-123-Metaiodobenzylguanidine imaging in patients with atrial fibrillation undergoing cardiac mapping and ablation of autonomic ganglia. Heart Rhythm 2017;14:128–32.

[31] Irie T, Yamakawa K, Hamon D, Nakamura K, Shivkumar K, Vaseghi M. Cardiac sympathetic innervation via middle cervical and stellate ganglia and antiarrhythmic mechanism of bilateral stellectomy. Am J Physiol Heart Circ Physiol 2017;312:H392–405.

[32] Dai M, Bao M, Zhang Y, et al. Low-level carotid baroreflex stimulation suppresses atrial fibrillation by inhibiting left stellate ganglion activity in an acute canine model. Heart Rhythm 2016;13:2203–12.

[33] Samuels MA. The brain-heart connection. Circulation 2007;116:77–84.

[34] Wang J, Chen Y, Li K, Hou L. Blockade of inhibitory neurotransmission evoked seizure-like firing of cardiac parasympathetic neurons in brainstem slices of newborn rats: Implications for sudden deaths in patients of epilepsy. Epilepsy Res 2006;70:172–83.

[35] Sakr YL, Lim N, Amaral AC, et al. Relation of ECG changes to neurological outcome in patients with aneurysmal subarachnoid hemorrhage. Int J Cardiol 2004;96:369–73.